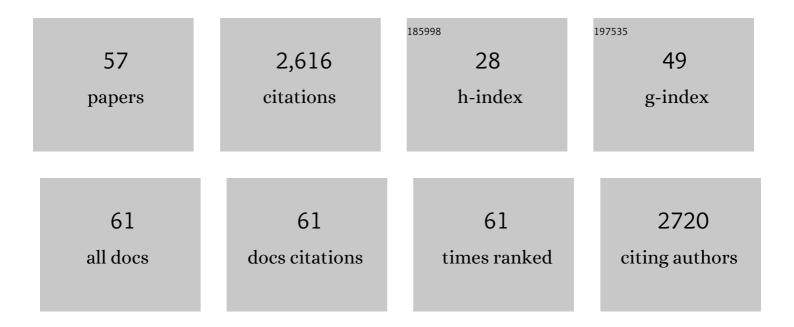
Stina Syvänen

List of Publications by Year in descending order

Source: https://exaly.com/author-pdf/6317724/publications.pdf Version: 2024-02-01



STINA SVUÃNEN

#	Article	IF	CITATIONS
1	¹¹ C-PiB and ¹²⁴ I-Antibody PET Provide Differing Estimates of Brain Amyloid-β After Therapeutic Intervention. Journal of Nuclear Medicine, 2022, 63, 302-309.	2.8	19
2	In vivo imaging of alpha-synuclein with antibody-based PET. Neuropharmacology, 2022, 208, 108985.	2.0	23
3	Passive and receptor mediated brain delivery of an anti-GFAP nanobody. Nuclear Medicine and Biology, 2022, 114-115, 128-134.	0.3	6
4	Advances in the development of new biomarkers for Alzheimer's disease. Translational Neurodegeneration, 2022, 11, 25.	3.6	65
5	PET Imaging in Preclinical Anti-AÎ ² Drug Development. Pharmaceutical Research, 2022, 39, 1481-1496.	1.7	7
6	Transferrin Receptor Binding BBB-Shuttle Facilitates Brain Delivery of Anti-Aβ-Affibodies. Pharmaceutical Research, 2022, , 1.	1.7	1
7	Reduction of αSYN Pathology in a Mouse Model of PD Using a Brain-Penetrating Bispecific Antibody. Pharmaceutics, 2022, 14, 1412.	2.0	12
8	Enhanced neprilysin-mediated degradation of hippocampal Aβ42 with a somatostatin peptide that enters the brain. Theranostics, 2021, 11, 789-804.	4.6	22
9	Pinpointing Brain TREM2 Levels in Two Mouse Models of Alzheimer's Disease. Molecular Imaging and Biology, 2021, 23, 665-675.	1.3	15
10	Wide-Ranging Effects on the Brain Proteome in a Transgenic Mouse Model of Alzheimer's Disease Following Treatment with a Brain-Targeting Somatostatin Peptide. ACS Chemical Neuroscience, 2021, 12, 2529-2541.	1.7	11
11	Brain pharmacokinetics of two BBB penetrating bispecific antibodies of different size. Fluids and Barriers of the CNS, 2021, 18, 26.	2.4	33
12	In vivo imaging of synaptic density with [11C]UCB-J PET in two mouse models of neurodegenerative disease. NeuroImage, 2021, 239, 118302.	2.1	19
13	Chemical imaging of evolving amyloid plaque pathology and associated Aβ peptide aggregation in a transgenic mouse model of Alzheimer's disease. Journal of Neurochemistry, 2020, 152, 602-616.	2.1	15
14	SPECT imaging of distribution and retention of a brain-penetrating bispecific amyloid-β antibody in a mouse model of Alzheimer's disease. Translational Neurodegeneration, 2020, 9, 37.	3.6	32
15	Fluorine-18-Labeled Antibody Ligands for PET Imaging of Amyloid-β in Brain. ACS Chemical Neuroscience, 2020, 11, 4460-4468.	1.7	28
16	Brain delivery of biologics using a crossâ€species reactive transferrin receptor 1 VNAR shuttle. FASEB Journal, 2020, 34, 13272-13283.	0.2	37
17	Brain Distribution of Drugs: Pharmacokinetic Considerations. Handbook of Experimental Pharmacology, 2020, , 1.	0.9	8
18	Blocking of efflux transporters in rats improves translational validation of brain radioligands. EJNMMI Research, 2020, 10, 124.	1.1	12

Stina Syväen

#	Article	IF	CITATIONS
19	In Vivo Studies of Drug BBB Transport: Translational Challenges and the Role of Brain Imaging. Handbook of Experimental Pharmacology, 2020, , 1.	0.9	1
20	Engineered antibodies: new possibilities for brain PET?. European Journal of Nuclear Medicine and Molecular Imaging, 2019, 46, 2848-2858.	3.3	49
21	Long-Term Effects of Traumatic Brain Injury in a Mouse Model of Alzheimer's Disease. Journal of Alzheimer's Disease, 2019, 72, 161-180.	1.2	18
22	Pyroglutamation of amyloid-βx-42 (Aβx-42) followed by Aβ1–40 deposition underlies plaque polymorphism in progressing Alzheimer's disease pathology. Journal of Biological Chemistry, 2019, 294, 6719-6732.	1.6	49
23	High detection sensitivity with antibody-based PET radioligand for amyloid beta in brain. NeuroImage, 2019, 184, 881-888.	2.1	50
24	Astroglial Responses to Amyloid-Beta Progression in a Mouse Model of Alzheimer's Disease. Molecular Imaging and Biology, 2018, 20, 605-614.	1.3	51
25	Intact blood-brain barrier transport of small molecular drugs in animal models of amyloid beta and alpha-synuclein pathology. Neuropharmacology, 2018, 128, 482-491.	2.0	29
26	Synthesis and preliminary preclinical evaluation of fluorine-18 labelled isatin-4-(4-methoxyphenyl)-3-thiosemicarbazone ([18F]4FIMPTC) as a novel PET tracer of P-glycoprotein expression. EJNMMI Radiopharmacy and Chemistry, 2018, 3, 11.	1.8	4
27	Blood-brain barrier integrity in a mouse model of Alzheimer's disease with or without acute 3D6 immunotherapy. Neuropharmacology, 2018, 143, 1-9.	2.0	27
28	Efficient clearance of Aβ protofibrils in AβPP-transgenic mice treated with a brain-penetrating bifunctional antibody. Alzheimer's Research and Therapy, 2018, 10, 49.	3.0	49
29	Antibody-Based In Vivo PET Imaging Detects Amyloid-β Reduction in Alzheimer Transgenic Mice After BACE-1 Inhibition. Journal of Nuclear Medicine, 2018, 59, 1885-1891.	2.8	32
30	A bispecific Tribody PET radioligand for visualization of amyloid-beta protofibrils – a new concept for neuroimaging. NeuroImage, 2017, 148, 55-63.	2.1	39
31	Combined PET and microdialysis for in vivo estimation of drug blood-brain barrier transport and brain unbound concentrations. Neurolmage, 2017, 155, 177-186.	2.1	25
32	Brain mGluR5 in mice with amyloid beta pathology studied with inÂvivo [11C]ABP688 PET imaging and exÂvivo immunoblotting. Neuropharmacology, 2017, 113, 293-300.	2.0	25
33	Delineating Amyloid Plaque Associated Neuronal Sphingolipids in Transgenic Alzheimer's Disease Mice (tgArcSwe) Using MALDI Imaging Mass Spectrometry. ACS Chemical Neuroscience, 2017, 8, 347-355.	1.7	66
34	Cationization increases brain distribution of an amyloid-beta protofibril selective F(ab')2 fragment. Biochemical and Biophysical Research Communications, 2017, 493, 120-125.	1.0	30
35	Pharmacokinetics, biodistribution and brain retention of a bispecific antibody-based PET radioligand for imaging of amyloid-β. Scientific Reports, 2017, 7, 17254.	1.6	39
36	Efficient and inexpensive transient expression of multispecific multivalent antibodies in Expi293 cells. Biological Procedures Online, 2017, 19, 11.	1.4	68

Stina Syväen

#	Article	IF	CITATIONS
37	Bivalent Brain Shuttle Increases Antibody Uptake by Monovalent Binding to the Transferrin Receptor. Theranostics, 2017, 7, 308-318.	4.6	146
38	Probing amyloidâ€Î² pathology in transgenic Alzheimer's disease (tgArcSwe) mice using <scp>MALDI</scp> imaging mass spectrometry. Journal of Neurochemistry, 2016, 138, 469-478.	2.1	34
39	Antibody-based PET imaging of amyloid beta in mouse models of Alzheimer's disease. Nature Communications, 2016, 7, 10759.	5.8	155
40	(R)-[11C]PK11195 brain uptake as a biomarker of inflammation and antiepileptic drug resistance: Evaluation in a rat epilepsy model. Neuropharmacology, 2014, 85, 104-112.	2.0	37
41	[11C]quinidine and [11C]laniquidar PET imaging in a chronic rodent epilepsy model: Impact of epilepsy and drug-responsiveness. Nuclear Medicine and Biology, 2013, 40, 764-775.	0.3	22
42	Advances in PET Imaging of P-Glycoprotein Function at the Blood-Brain Barrier. ACS Chemical Neuroscience, 2013, 4, 225-237.	1.7	64
43	Specific Uptake of an Amyloid-β Protofibril-Binding Antibody-Tracer in AβPP Transgenic Mouse Brain. Journal of Alzheimer's Disease, 2013, 37, 29-40.	1.2	65
44	Altered GABA _A Receptor Density and Unaltered Blood–Brain Barrier Transport in a Kainate Model of Epilepsy: An In Vivo Study Using ¹¹ C-Flumazenil and PET. Journal of Nuclear Medicine, 2012, 53, 1974-1983.	2.8	26
45	Alteration in P-glycoprotein Functionality Affects Intrabrain Distribution of Quinidine More Than Brain Entry—A Study in Rats Subjected to Status Epilepticus by Kainate. AAPS Journal, 2012, 14, 87-96.	2.2	24
46	Synthesis and preclinical evaluation of [11C]D617, a metabolite of (R)-[11C]verapamil. Nuclear Medicine and Biology, 2012, 39, 530-539.	0.3	16
47	Pharmacokinetic modeling of P-glycoprotein function at the rat and human blood–brain barriers studied with (R)-[11C]verapamil positron emission tomography. EJNMMI Research, 2012, 2, 58.	1.1	16
48	[11C]phenytoin revisited: synthesis by [11C]CO carbonylation and first evaluation as a P-gp tracer in rats. EJNMMI Research, 2012, 2, 36.	1.1	28
49	[11C]Flumazenil brain uptake is influenced by the blood-brain barrier efflux transporter P-glycoprotein. EJNMMI Research, 2012, 2, 12.	1.1	16
50	Simultaneous in vivo measurements of receptor density and affinity using [11C]flumazenil and positron emission tomography: Comparison of full saturation and steady state methods. NeuroImage, 2011, 57, 928-937.	2.1	9
51	(R)-[11C]Verapamil PET studies to assess changes in P-glycoprotein expression and functionality in rat blood-brain barrier after exposure to kainate-induced status epilepticus. BMC Medical Imaging, 2011, 11, 1.	1.4	43
52	Using PET Studies of P-gp Function to Elucidate Mechanisms Underlying the Disposition of Drugs. Current Topics in Medicinal Chemistry, 2010, 10, 1799-1809.	1.0	28
53	Species Differences in Blood-Brain Barrier Transport of Three Positron Emission Tomography Radioligands with Emphasis on P-Glycoprotein Transport. Drug Metabolism and Disposition, 2009, 37, 635-643.	1.7	305
54	On The Rate and Extent of Drug Delivery to the Brain. Pharmaceutical Research, 2008, 25, 1737-1750.	1.7	425

Stina Syväen

#	Article	IF	CITATIONS
55	Pharmacokinetics of Pâ€glycoprotein inhibition in the rat bloodâ€brain barrier. Journal of Pharmaceutical Sciences, 2008, 97, 5386-5400.	1.6	26
56	Duration and degree of cyclosporin induced P-glycoprotein inhibition in the rat blood–brain barrier can be studied with PET. NeuroImage, 2006, 32, 1134-1141.	2.1	58
57	Pharmacokinetic Consequences of Active Drug Efflux at the Blood–Brain Barrier. Pharmaceutical Research, 2006, 23, 705-717.	1.7	57